Methodology for Minimizing Risk from Airborne Organisms in Hospital Isolation Rooms

Farhad Memarzadeh, Ph.D., P.E. **Jane Jiang, Ph.D.**

ABSTRACT

This paper compares the use of ultraviolet germicidal irradiaiton (UVGI) with increased ventilation flow rate to minimize the risk from airborne bacteria in hospital isolation rooms. Results show that the number of particles deposited on surfaces and vented out is greater in magnitude than the number killed by UV light and that the numbers for these two mechanisms are large compared to the total number of particles.

INTRODUCTION

The patients in hospital isolation rooms constantly produce transmissible airborne organisms by coughing, sneezing, or talking, which, if not under control, results in spreading airborne infection. Tuberculosis (TB) infection, for example, occurs after inhalation of a sufficient number of tubercle bacilli expelled during a cough by a patient (*Federal Register* 1993). The contagion depends on the rate at which bacilli are discharged, i.e., the number of the bacilli released from the infectious source. It also depends on the virulence of the bacilli as well as external factors, such as the ventilation flow rate. In order to prevent the transmission of airborne infection, the isolation rooms are usually equipped with high-efficiency ventilation systems operating at high supply flow rate to remove the airborne bacteria from the rooms. However, unexpected stagnant regions, or areas of poor mixing, mean that the ventilation rate is no guarantee of good control of the spreading of airborne infection.

Another means of minimizing the risk from airborne bacteria is to apply ultraviolet germicidal irradiation (UVGI). UVGI holds promise of greatly lowering the concentration of airborne bacteria and thus controlling the spread of airborne infection among occupants. Comparing the clearance level of airborne bacteria achieved by increased ventilation flow rate or by applying UVGI may be useful in evaluating the efficiency of UVGI.

The most widely used application of UVGI is in the form of passive upper-room fixtures containing UVGI lamps that irradiate a horizontal layer of airspace above the occupied zone. They are designed to kill bacteria that enter the upper irradiated zone and are highly reliant on vertical room air currents. The survival probability of bacteria after being exposed to UVGI depends on the UV irradiance as well as the exposure time in a general form (*Federal Register* 1993):

$$\% \, Survival = 100 \times e^{-kIt}, \quad (1)$$

where

I = UV irradiance, $\mu W/cm^2$,

t = time of UV exposure,

k = the microbe susceptibility factor, $cm^2/\mu W \cdot s$.

Increasing room air mixing enhances upper-room UVGI effectiveness by bringing more bacteria into the UV zone. However, rapid vertical air circulation also implies insufficient exposure time. It can be understood that removing and killing bacteria in isolation rooms are greatly influenced by the flow pattern of ventilation air through parameters such as:

- Ventilation flow rate
- Locations of air supplies/exhausts
- Supply air temperature
- Location of the UV fixture(s)
- Room configuration
- Susceptibility of the particular species of bacteria

Farhad Memarzadeh is chief of the Technical Resources Group at the National Institutes of Health, Bethesda, Md. **Jane Jiang** is with Flomerics, Inc., Marlboro, Mass.

In order to achieve a better performance of UVGI as well as a higher removal effectiveness of the ventilation system, the airflow pattern needs to be fully understood and well organized. Therefore, it is necessary to conduct a system study on minimizing the risk from airborne organisms in hospital isolation rooms with all the important parameters being analyzed.

Previous research has been almost entirely based on empirical methods (Chang et al. 1985; Macher et al. 1992; Mortimer and Hughes 1995), which are time consuming and are limited by the cost of modifying physical installations of the ventilation systems. The absence of UV treatment systems also imposed limitations on previous research. Therefore, the design guidance for isolation rooms basically relied on gross simplifications without fully understanding the effect of the complex interaction of room airflow and UV treatment systems.

Computational fluid dynamics (CFD, sometimes known as airflow modeling) has been proven to be very powerful and efficient in research projects involving parametric study of room airflow and contaminant dispersion (Jiang et al. 1997; Jiang et al. 1995; Haghighat et al. 1994). In addition, the output of the CFD simulation can be presented in many ways, for example, with the useful details of field distributions as well as overviews on the effects of parameters involved. Therefore, CFD is employed as a main approach in this study (FV 1995).

The results of this study are also intended to be linked to a concurrent study into thermal comfort, uniformity, and ventilation effectiveness in patient rooms. While the patient room is not exactly the same in terms of dimensions, the two studies share enough common features—for example, there is a single bed in the room, the glazing features are similar in each case, there are similar amounts of furniture in the room, etc.—that the conclusions drawn from the patient room study will be viable in this study, and vice versa.

PURPOSE OF THIS STUDY

Following are the main purposes of the study presented here.

1. Use airflow modeling to evaluate the effects of some of the parameters listed above, such as
   - ventilation flow rate,
   - supply temperature,
   - exhaust location, and
   - baseboard heating (in winter scenarios),

   on minimizing the risk from airborne organisms in isolation rooms. Other factors, such as the location and number of the UV fixtures, are being addressed in further research.
2. Assess the effectiveness of
   - removing bacteria via the ventilation system, either through the particles sticking to the wall or by ventilation through exhaust grilles, and
   - killing bacteria with UV.
3. Provide an architectural/engineering tool for good design practice that is generally applicable to conventional isolation room use.

METHODOLOGY

Airflow Modeling

Airflow modeling based on computational fluid dynamics (CFD) (FV 1995), which solves the fundamental conservation equations for mass momentum and energy in the form of the Navier-Stokes equations, is now well established:

$$\frac{\partial}{\partial t}(\rho\varphi) + div(\rho\vec{V}\varphi - \Gamma_{\varphi}\text{grad}\,\varphi) = S_{\varphi} \qquad (2)$$

Transient + Convection – Diffusion = Source

where

ρ = density,

$\vec{V}$ = velocity vector,

φ = dependent variable,

Γ_{φ} = exchange coefficient (laminar + turbulent),

S_{φ} = source or sink.

How Is It Done? Airflow modeling solves the set of Navier Stokes equations by superimposing a grid of many tens or even hundreds of thousands of cells that describe the physical geometry, heat, contamination sources, and the air itself. Figures 1 and 2 show a typical research laboratory and the corresponding space discretization, subdividing the laboratory into the cells. In this study, a finite-volume approach was used to consider the discretization and solution of the equations.

The simultaneous equations thus formed are solved iteratively for each one of these cells to produce a solution that satisfies the conservation laws for mass, momentum, and energy. As a result, the flow can then be traced in any part of

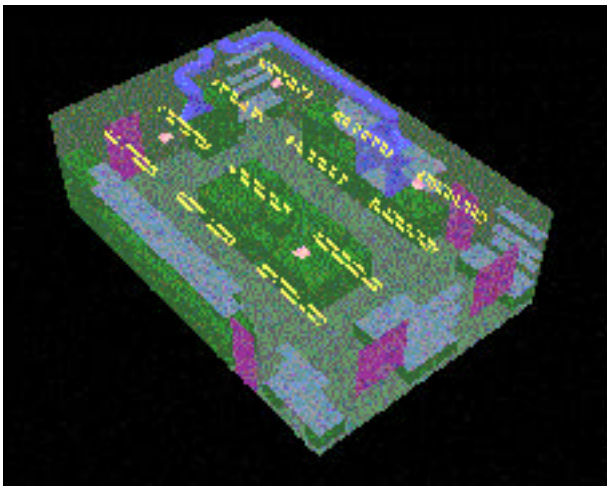

Figure 1 *Geometric model of a laboratory.*

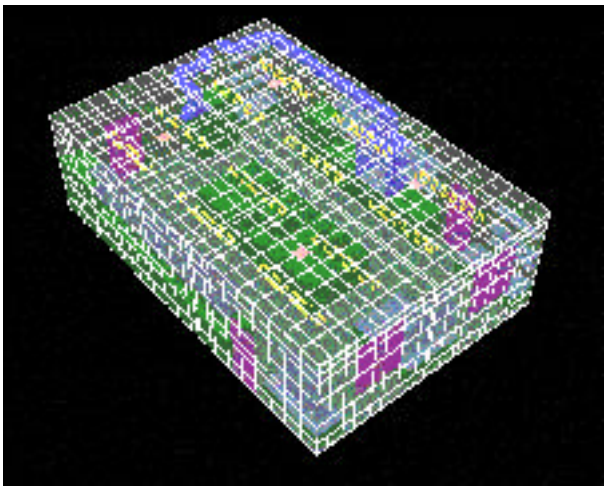

Figure 2 *Superimposed grid of cells for calculation.*

the room simultaneously, coloring the air according to another parameter such as temperature.

Due to the nature of the particle tracking algorithm used in this study, the turbulence model used was the *k*-ε turbulence model. Further, the *k*-ε turbulence model represented the most appropriate choice of model because of its extensive use in other research applications. No other turbulence model has been developed that is as universally accepted.

Validation of Airflow Modeling Methodology. The methodology and most of the results generated in this paper have been or are under peer review by numerous entities. The methodology was also used extensively in a previous publication by Memarzadeh (1998), which considered ventilation design on animal research facilities using static microisolators. In order to analyze the ventilation performance of different settings, numerical methods based on computational fluid dynamics were used to create computer simulations of more than 160 different room configurations. The performance of this approach was successfully verified by comparison with an extensive set of experimental measurements. A total of 12.9 million experimental data values were collected to confirm the methodology. The average errors between the experimental and computational values were 14.36% for temperature and velocities, while the equivalent value for concentrations was 14.50%.

To further this research, several progress meetings were held to solicit project input and feedback from the participants. There were more than 55 international experts on all facets of the animal care and use community, including scientists, veterinarians, engineers, animal facility managers, and cage and rack manufacturers. The pre-publication project report underwent peer review by a ten-member panel from the participant group, selected for their expertise in pertinent areas. Their comments were adopted and incorporated in the final report.

The publication was reviewed by a technical committee of the American Society of Heating, Refrigerating and Air-Conditioning Engineers (ASHRAE) and data accepted for inclusion in their 1999 Handbook.

Simulation of Bacteria Droplets

Basic Concept. The basic assumption in this study is that the droplet carrying the bacteria colony can be simulated as particles being released from several sources surrounding the occupant. These particles then are tracked for a certain period of time in the room. The evaporation experienced by the droplet is not simulated in this study. No research literature could be found that defined the evaporation of the droplet subject to the UV dosage. However, in numerical tests in which the particle diameter was reduced from 1 mm (used as the representative particle diameter) to 0.1 mm, the effect was seen to be relatively small (<10%). The dose that the particles received when traveling in the room along their trajectories is the summation of the dose received at each time-step, calculated as

$$Dose = \Sigma\,(dt \cdot I) \tag{3}$$

where dt is the time step and I is the local UV irradiance. Then, based on the dose received, the survival probability of each particle is evaluated.

Since the airflow in a ventilated room is turbulent, the bacteria from coughing or sneezing of the occupants in the room are transported not only by convection of the airflow but also by the turbulent diffusion. The bacteria are light enough, and in small enough quantities, that they can be considered not to exert an influence on airflow. Therefore, from the output of the CFD simulation, the distributions of air velocities and the turbulent parameters can be directly applied to predict the path of the airborne bacteria in convection and diffusion processes.

Particle Trajectories. The methodology for predicting turbulent particle dispersion used in this study was originally devised by Gosman and Ioannides (1981) and validated by Ormancey and Martinon (1984), Shuen et al. (1983), and Chen and Crowe (1984). Experimental validation data were obtained from Snyder and Lumley (1971). Turbulence was incorporated into the Stochastic model via the *k*-ε turbulence model (Alani et al. 1998).

The particle trajectories are obtained by integrating the equation of motion in three coordinates. Assuming that body forces are negligible, with the exception of drag and gravity, these equations can be expressed as follows:

$$m_p \frac{du_p}{dt} = \frac{1}{2} C_D A_p \rho (u - u_p) \sqrt{(u - u_p)^2 + (v - v_p)^2 + (w - w_p)^2} + m_p g_x \tag{4.1}$$

$$m_p \frac{dv_p}{dt} = \frac{1}{2} C_D A_p \rho (v - v_p) \sqrt{(u - u_p)^2 + (v - v_p)^2 + (w - w_p)^2} + m_p g_y \tag{4.2}$$

$$m_p \frac{dw_p}{dt} = \frac{1}{2} C_D A_p \rho (w - w_p) \sqrt{(u - u_p)^2 + (v - v_p)^2 + (w - w_p)^2} + m_p g_z \quad (4.3)$$

$$\frac{dx_p}{dt} = u_p \quad (5.1)$$

$$\frac{dy_p}{dt} = v_p \quad (5.2)$$

$$\frac{dz_p}{dt} = w_p \quad (5.3)$$

where

u, v, w = instantaneous velocities of air in x, y, and z directions,
u_p, v_p, w_p = particle velocity in x, y, and z directions,
x_p, y_p, z_p = particle moving in x, y, and z directions,
g_x, g_y, g_z = gravity in x, y, and z directions,
A_p = cross-sectional area of the particle,
m_p = mass of the particle,
ρ = density of the particle,
C_D = drag coefficient,
dt = time interval.

The drag coefficient for a spherical particle, taken from Wallis (1969), is

$$C_D = \frac{24}{\mathrm{Re}}\left(1 + \frac{3}{16}\mathrm{Re}\right)^{0.5}, \text{ for } \mathrm{Re} \le 1000, \quad (6)$$

and

$$C_D = 0.44, \text{ for } \mathrm{Re} > 1000. \quad (7)$$

The Reynolds number of the particle is based on the relative velocity between particle and air.

In laminar flow, particles released from a point source with the same weight would initially follow the airstream in the same path and then fall under the effect of gravity. Unlike in laminar flow, the random nature of turbulence indicates that the particles released from the same point source will be randomly affected by turbulent eddies. As a result, they will be diffused away from the streamline at different fluctuating levels. In order to model the turbulent diffusion, the instantaneous fluid velocities in the three Cartesian directions, u, v, and w, are decomposed into the mean velocity component and the turbulent fluctuating component as follows:

$$u = \bar{u} + u', v = \bar{v} + v', w = \bar{w} + w'$$

where $\bar{u}$ and u' are the mean and fluctuating components in the x direction. The same applies for the y and z directions. The stochastic approach prescribes the use of a random number generator algorithm, which, in this case, is taken from Press et al. (1992) to model the fluctuating velocity. It is achieved through using a random sampling of a Gaussian distribution with a mean of 0 and a standard deviation of unity. Assuming homogeneous turbulence, the instantaneous velocities of air are then calculated from kinetic energy of turbulence:

$$u = \bar{u} + N\alpha \quad (8.1)$$

$$v = \bar{v} + N\alpha \quad (8.2)$$

$$w = \bar{w} + N\alpha \quad (8.3)$$

where N is the pseudo-random number, ranging from 0 to1, with

$$\alpha = (2k/3)^{0.5}, \quad (9)$$

and k is the turbulent kinetic energy.

The mean velocity, which is the direct output of CFD, determines the convection of the particles along the streamline, while the turbulent fluctuating velocity, $N\alpha$, contributes to the turbulent diffusion of the particle.

Particle Interaction Time. With the velocities known, the only component needed for calculating the trajectory is the time interval (t_{int}) over which the particle interacts with the turbulent flow field. The concept of turbulence being composed of eddies is employed here. Before determining the interaction time, two important time scales need to be introduced: the eddy's time scale and the particle transient time scale.

Eddy's time scale: the lifetime of an eddy, defined as

$$t_e = \left(\frac{l_e}{|N\alpha|}\right) \quad (10)$$

where

$$l_e = \frac{C\mu\, k^{3/2}}{\varepsilon} \quad (11)$$

l_e = dissipation length scale of the eddy,
k = turbulent kinetic energy,
ε = dissipation rate of turbulent kinetic energy,
$C\mu$ = a constant in the turbulence model.

The transient time scale for the particle to pass through the eddy, t_r, is estimated as

$$t_r = -\tau \ln\left\{1.0 - \frac{l_e}{\tau\left|\left(\sqrt{\bar{u}^2 + \bar{v}^2 + \bar{w}^2}\right) - \left((u_p)^2 + (v_p)^2 + (w_p)^2\right)\right|}\right\} \quad (12)$$

and

$$\tau = \frac{\frac{4}{3}\rho_p D}{\left\{\rho C_D\left|\left(\sqrt{\bar{u}^2 + \bar{v}^2 + \bar{w}^2}\right) - \left((u_p)^2 + (v_p)^2 + (w_p)^2\right)\right|\right\}} \quad (13)$$

where τ is the particle relaxation time, indicating the time required for a particle starting from rest to reach 63% of the flowing stream velocity. D is the diameter of the particle.

The interaction time is determined by the relative importance of the two events. If the particle moves slowly relative

to the gas, it will remain in the eddy during the whole lifetime of the eddy, t_e. If the relative velocity between the particle and the gas is appreciable, the particle will transverse the eddy in its transient time, t_r. Therefore, the interaction time is the minimum of the two:

$$t_{int} = min(t_e, t_r) \quad (14)$$

In this study, the interaction time is on the order of 1e-5 to 1e-6 s. If the particle track time is set to 300 s, some 60,000,000 time steps need to be performed just to calculate the trajectory for one particle.

Testing of Particle Tracking Methodology. A simple test configuration was defined to confirm that the particle tracking methodology was functioning as intended. There are many aspects to be investigated, including inertial, gravitational, and slip effects, but in particular the simulations shown here were intended to test that the wall interaction worked correctly. The test was specified to incorporate typical flow and blockage effects present in the isolation room, in particular an inlet (supply), openings (vents), and a block in the flow path (internal geometry and obstructions).

The geometry of the test configuration is shown in Figure 3. The configuration had dimensions of 0.5 m (20 in.) × 0.5 m (20 in.) × 1.0 m (40 in.). It contained a 0.5 m (20 in.) × 0.5 m (20 in.) supply at one end, through which the flow rate was varied, and an opening of half that size at the other end. An additional opening of dimensions 0.1 m (4 in.) × 0.5 m (20 in.) was also included approximately halfway along the section. Both openings were defined as representing atmospheric conditions: no flow rate was defined through the openings. The final item in the configuration was a block of dimensions 0.5 m (20 in.) × 0.5 m (20 in.) × 0.25 m (10 in.), which was included to represent a typical obstruction.

In the tests, 20 particles were released with even spacing across the center of the inlet supply. The test particles were 1 mm in diameter, with a density of 1000 kg/m^3. In terms of supply conditions, two different flow rates were considered: 0.25 kg/s (445 cfm) and 1.0 kg/s (1780 cfm). Different coordinate orientations were considered to evaluate whether coordinate biasing existed. In particular, the configuration was considered with the supply in the positive and negative *x*, *y*, and *z* directions. With the two different flow rates considered, 12 cases were run to test the particle tracking methodology.

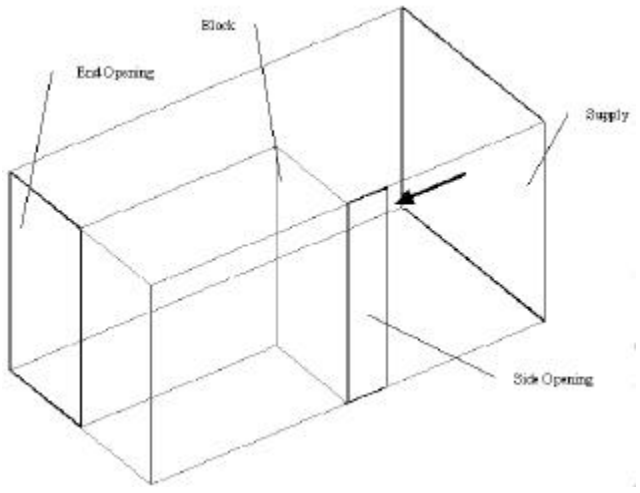

Figure 3 *Geometry of test configuration.*

The results of a typical case are shown in Figure 4, in particular, the positive *x* orientation at 0.25 kg/s (445 cfm). The solid lines represent the particle tracks. The following can be seen clearly from the figure:

- The majority of the particles exit through the end or side openings.
- Relatively few particles (two or three) impinge on the internal block or side walls.

These features are also exhibited by all the other cases. Based on the results from these tests, the particle tracking methodology can be seen to be working correctly.

Calculation Procedure

The calculation procedure for each case consists of four steps:

1. Computing the field distribution of fluid velocity, temperature, and turbulent parameters.
2. Adding the UV distribution into the result field with the specified fixture location and measurement data.
3. Specifying the source locations from where a specified number of particles are released. Note that the particles are not continuously released; they are released from the source locations only at the start of the analysis period, i.e., $t = 0$ s.
4. Performing computational analysis to calculate trajectory for each particle for up to 300 s from initial release. The output of the analysis includes:
    - The number of particles being removed by ventilation varying with time (for every 60 s).
    - The number of viable particles varying with time (for every 60 s).
    - The number of particles killed by UV dosage varying with time (for every 60 s).
    - The percentage of surviving particles in the room varying with time (for every 60 s).
    - The number of particles in different dose bands (for every 60 s).

MODEL SETUP

CFD Models

Figure 5 shows the configuration of the isolation suite being studied. The suite consists of three rooms, connected through the door gaps between them: the main isolation room, the bathroom, and the vestibule. The main room is equipped with four slot diffusers near the window and a low induction diffuser on the ceiling.

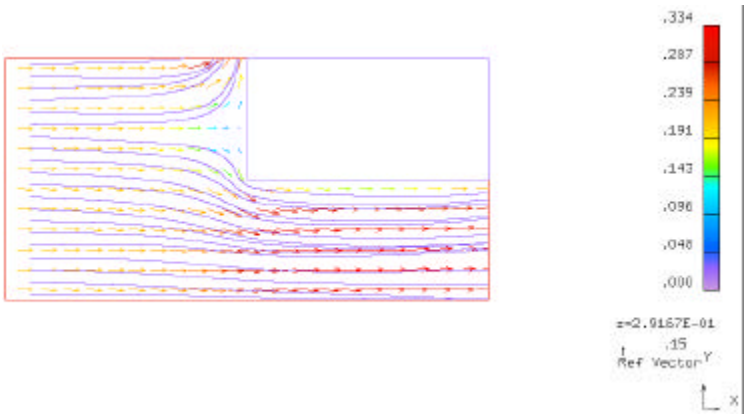

Figure 4 *Test results for positive × direction, 0.25 kg/s (445 cfm) case.*

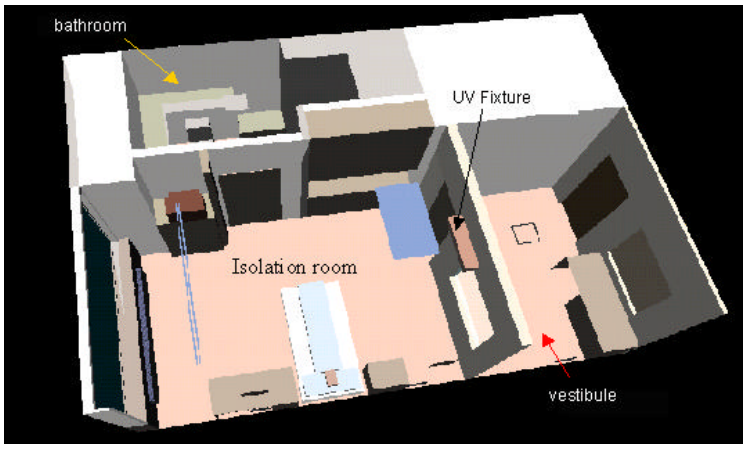

Figure 5 *Configuration of the isolation suite.*

Three extreme weather conditions that affect the supply temperature are considered:

- Peak Load: Maximum summer day solar loading for south-facing isolation room. External temperature is 31.5°C (88.7°F).
- Peak T: Maximum summer day external temperature 35°C (95°F) without solar radiation in the room.
- Minimum T: Minimum winter night temperature of –11.7°C (10.9°F).

In the peak load scenarios, the transmitted portion of the solar flux through the window was included, and the absorbed fraction was added directly to the glazing. Radiation from the glazing was also included in the cases. As the room is considered to be surrounded by rooms of similar build and configuration, all the walls, the ceiling, and the floor are considered adiabatic, except for the wall that is in contact with the external conditions and so subject to heat loss/ gain. In all cases considered, the heat dissipated by the patient was included. Other heat gains in the room included lamps, a television, lighting, and miscellaneous items usually found in isolation rooms, for example, heating pads, equipment, etc.

The variation of the ventilation parameters involves:

- Supply flow rate (2-16 ACH)
- Weather condition: summer or winter (supply temperature)
- Ventilation system:
    - Low exhausts
    - High exhausts
    - Low exhausts with baseboard heating for winter cases

Twenty cases with two low exhausts in the isolation room, as listed in Table 1, were studied to evaluate the influence of the supply flow rate and temperature on the particle tracking. In order to examine the effects of ventilation system change, ten cases were run with high exhausts and the combination of baseboard heating and low exhausts (see Table 2). Figure 6 shows the locations of the diffusers, exhausts, and the baseboard heating in the main room. The baseboard heater used was 7.9 ft (2.4 m) long and 18 in. (0.46 m) high and accounted for 80% of the heating required in the extreme winter case. In particular, the heater dissipated 396 W total, or 171.1 Btu/h·ft (165 W/m).

The UV lamp fixture is located on the partition wall between the isolation room and the vestibule 7.5 ft (2.29 m) from the floor with a total lamp rating of 36 W (10 W UV

TABLE 1
Twenty Cases with Variation in Supply Flow Rate and Temperature

Case	Weather Condition	ACH	Main Isol. Room (cfm)		Bathroom (cfm)		Vestibule (cfm)		Supply Temp. (°C)
			Sup.	Exh.	Sup.	Exh.	Sup.	Exh.	
Case 1	Min. T	2	62	42	0	100	180	150	37.2
Case 2	Peak T	4	125	105	"	"	"	"	9.2
Case 3	Min. T	"	"	"	"	"	"	"	30
Case 4	Peak T	6	187	167	"	"	"	"	13.8
Case 5	Min. T	"	"	"	"	"	"	"	27.7
Case 6	Peak load	8	250	230	0	"	"	"	9.6
Case 7	Peak T	"	"	"	"	"	"	"	16.1
Case 8	Min. T	"	"	"	"	"	"	"	26.5
Case 9	Peak load	10	312	292	0	"	"	"	12.2
Case 10	Peak T	"	"	"	"	"	"	"	17.5
Case 11	Min. T	"	"	"	"	"	"	"	25.8
Case 12	Peak load	12	375	355	0	"	"	"	14
Case 13	Peak T	"	"	"	"	"	"	"	18.4
Case 14	Min. T	"	"	"	"	"	"	"	25.3
Case 15	Peak load	14	437	417	0	"	"	"	15.3
Case 16	Peak T	"	"	"	"	"	"	"	19.1
Case 17	Min. T	"	"	"	"	"	"	"	25
Case 18	Peak load	16	499	479	0	"	"	"	16.3
Case 19	Peak T	"	"	"	"	"	"	"	19.5
Case 20	Min. T	"	"	"	"	"	"	"	24.8

TABLE 2
Ten Cases with Variation of Ventilation System

Case	Weather Condition	ACH	Main Isol. Room (cfm)		Bathroom (cfm)		Vestibule (cfm)		Supply Temp (°C)	Change in Ventilation System
			Sup.	Exh.	Sup.	Exh.	Sup.	Exh.		
Case 21	Min. T	2	62	42	0	100	180	150	25.8	Baseboard heating
Case 22	"	6	187	167	"	"	"	"	23.9	"
Case 23	"	12	375	355	"	"	"	"	23.5	"
Case 24	"	16	499	479	"	"	"	"	23.3	"
Case 25	Peak T	4	125	105	"	"	"	"	9.2	High exhausts in main room
Case 26	Min. T	"	"	"	"	"	"	"	30	"
Case 27	Peak T	10	312	292	"	"	"	"	17.5	"
Case 28	Min. T	"	"	"	"	"	"	"	25.8	"
Case 29	Peak T	16	499	479	"	"	"	"	19.5	"
Case 30	Min. T	"	"	"	"	"	"	"	24.8	"

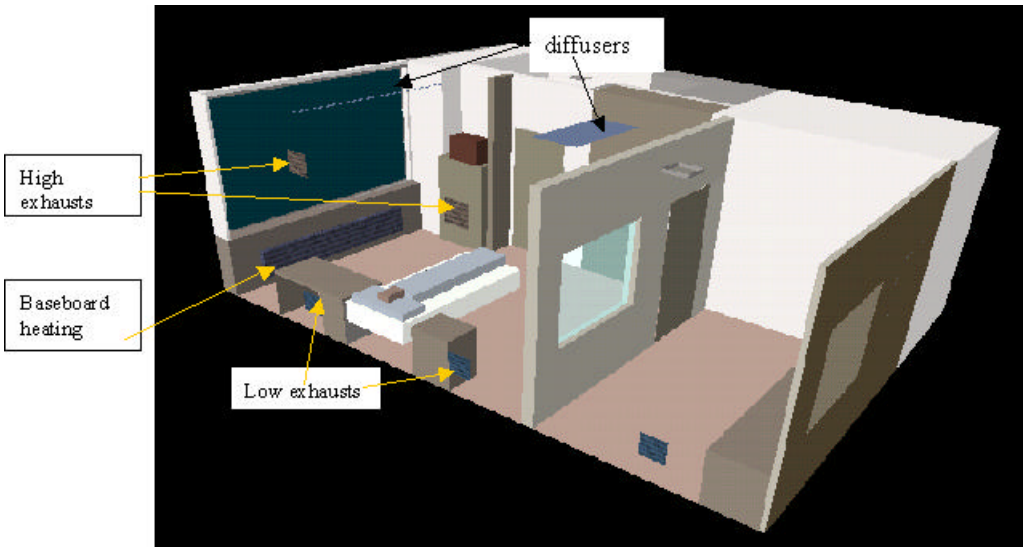

Figure 6 *Ventilation system in the isolation room.*

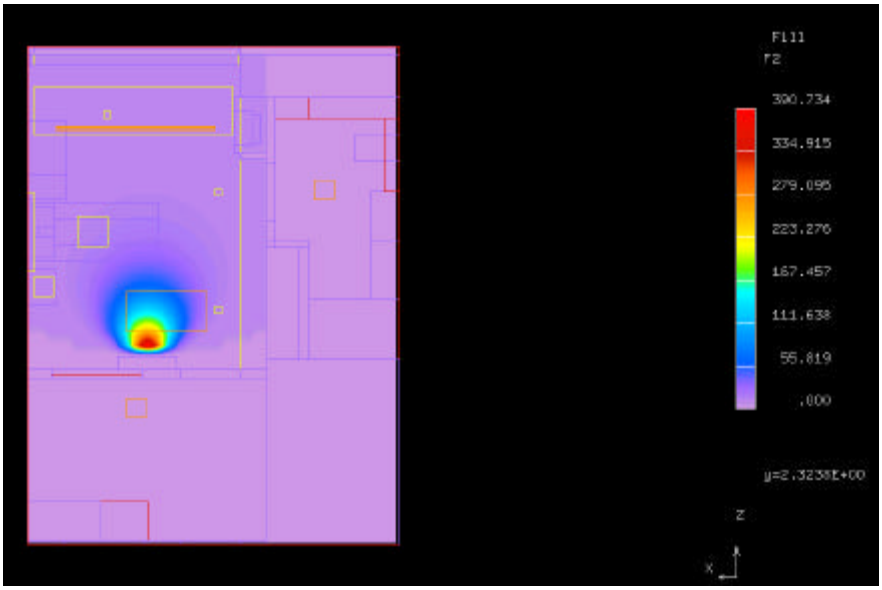

Figure 7 *Plan view of UV field through lamp. Values in* $\mu W/cm^2$.

output). The plan view of the UV field generated by the lamp is shown in Figure 7. The UV intensity is assumed to be constant over the 5 in. (1.27e-2 m) height of the lamp. The heat dissipated was not considered in the cases, as it spread over a wide volume within the room and represents only a small fraction of the heat budget in the room.

The location and intensity of the lamps were also considered as a parameter for a limited subset of cases for comparison. Here, the location of the lamp was changed to be immediately above the bed, while the effective UV output was doubled, then quadrupled, from the original value, i.e., 20 W and 40 W, respectively.

Great care was taken with regard to the correct representation of the diffusers in the room, as well as the numerical grid used. The numerical diffuser models were validated against available manufacturers' data to ensure that throw characteristics were matched accurately. This was performed for all the diffuser types (linear slot, low induction, and four-way diffuser) and for an appropriate range of flow rates.

The number of grid cells used in these cases was on the order of 370,000 cells. Grid dependency tests were performed to ensure that the results were appropriate and would not vary on increasing the grid density. In particular, attention in the tests was directed at the areas containing the main flow or heat sources in the room, for example, the diffusers and the area close to the glazing, as well as areas of largest flow or temperature gradients, for example, the area close to the baseboard

heating and the flow through the door cracks. Grid was added appropriately in these regions and their surroundings until grid independence was achieved.

Model for Bacteria Killing

The bacteria are simulated as 100 particles released from 27 discrete source locations above the bed in a 3 × 3 × 3 array. The distance between the array release points in the vertical direction was 3 ft (0.91 m). The particles are not continuously released; they are released from the source locations only at the start of the analysis period, i.e., $t = 0$ s. The 2700 particles were tracked for 300 s from initial release or until they were removed from the room by the ventilation system or stuck to the wall.

The percentage survival is dependent on exposure to UV dose, defined as

$$Dose = Exposed\ time \cdot UV\ Irradiance, \quad (15)$$

in different patterns due to the room condition, the relative humidity, and the susceptibility of the species of the bacteria. In this report, the probability of survival was calculated using the empirical equation illustrated in Figure 8:

$$PS = a * \exp(-k\,x) \quad (16)$$

$$a = 100$$

$$k = 0.00384$$

where

a = coefficient from curve fitting,
PS = survival probability,
x = UV dose,
k = susceptibility.

Model for Impingement of Particles on Solid Surfaces

In the particle tracking methodology outlined above, a particle would hit a surface because of the addition of the turbulent fluctuation velocity component to the particle trajectory.

When the particles hit a wall surface, they may stick on or "bounce" away from the surface depending on a variety of influences, such as electric force, molecular force, surface roughness, and temperature, and the fact that the cough particles are essentially aerosol in nature. In order to represent the influences, a probability should be introduced dependent on the conditions. However, there is no current research information available that is applicable to the particle conditions in this study. Two models were therefore considered in this study, a non-stick model, in which particles were prevented from depositing on wall surfaces, and a stick model, in which wall deposition was considered.

As will be shown in the results, the primary conclusions made in the study are applicable to both deposition models. The primary reason for this is that particles that have trajectories that take them close to surfaces necessarily move into low velocity regions close to the surfaces. In these near wall regions, the particles are generally not affected by the ventilation system and therefore behave in a way similar to deposited particles in the analysis.

The results presented in the following section are generally with the non-stick model imposed. A comparison of the non-stick and stick model will be presented as well.

RESULTS

The results are presented in graphical format showing the status of the 2700 particles for the tracking period considered (300 s). Tests were performed for other particle track times for

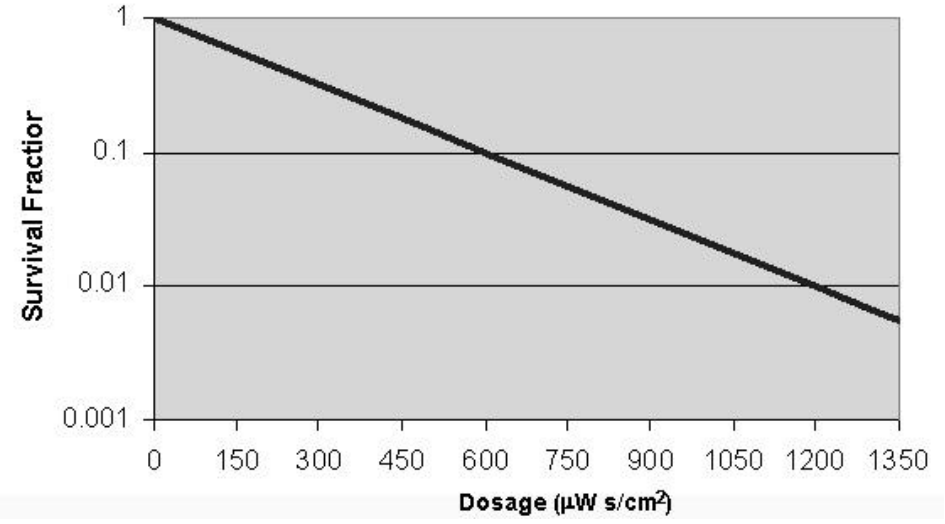

Figure 8 *Survival fraction vs. dosage for* M. tuberculosis *(First et al. 1999).*

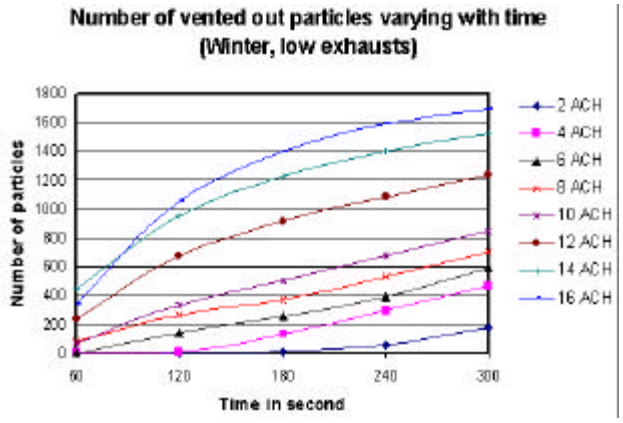

Figure 9 *Number of vented out particles with ACH change (winter).*

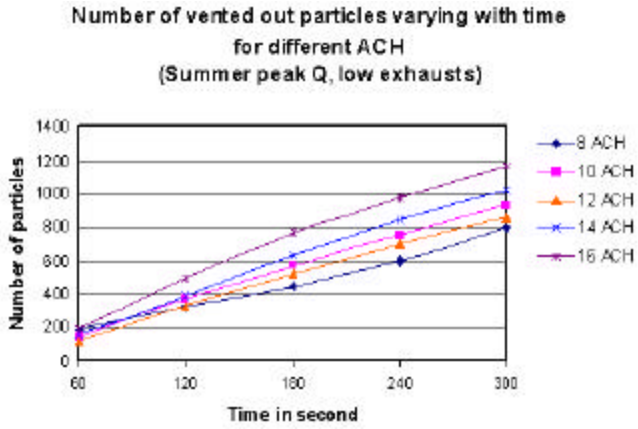

Figure 10 *Number of vented out particles with ACH change (summer).*

different cases; in particular, tests were performed with track times of three, five, and ten minutes. The variation from run to run was not significant. The particle status indicates the removal effectiveness of the ventilation system and UVGI. There are three particle statuses considered here:

- Status 1—Vented out (considered eliminated)
- Status 2—Killed by UV (killed)
- Status 3—Not killed (viable)

The results from the particle tracking are presented in 15 charts showing:

- The number of particles being removed by ventilation, varying with time (for every 60 s)
- The number of viable particles varying with time (for every 60 s)
- The number of particles killed by UV dosage, varying with time (for every 60 s)
- The survival fraction of particles, varying with time (for every 60 s)
- Comparison of the stick and non-stick models

Number of Particles Removed by Ventilation

Figures 9 to 11 show the number of particles removed by ventilation, varying with time, for several parametrical changes. Figures 9 and 10 show the variation with ACH for the winter (with no baseboard heating) and summer conditions, respectively. The winter cases (Figure 9) show a bigger variation in the number of ventilated particles than the summer cases. This is because there is generally poorer mixing for winter cases with no baseboard heating than for summer cases.

Figure 11 shows the variation in vented particles with time based on exhaust location. The result indicates that the high level exhaust is generally more effective than the low level exhausts in removing particles through ventilation for the particle release points considered in this study. However, this trend is reversed at the higher ACH considered.

Number of Viable Particles Varying with Time

Figures 12 to 15 show the number of viable particles varying with time for several parametrical changes. The winter cases with no baseboard heating (Figure 12) show a bigger variation in the number of viable particles than the summer cases. The main reason for this result can again be traced to the poor mixing conditions for the winter cases with no baseboard heating. In particular, the particles are less likely to be removed through ventilation or killed by UV dosage because of the mixing.

Figure 13 shows the clear benefit in the inclusion of baseboard heating. In particular, the inclusion of baseboard heat at 2 ACH results in similar viable particle numbers to much higher ACH values without baseboard heating.

A point of interest here is the connection between Figure 14 and the concurrent study on the thermal comfort and uniformity in a typical patient room. Figure 14 shows that there is

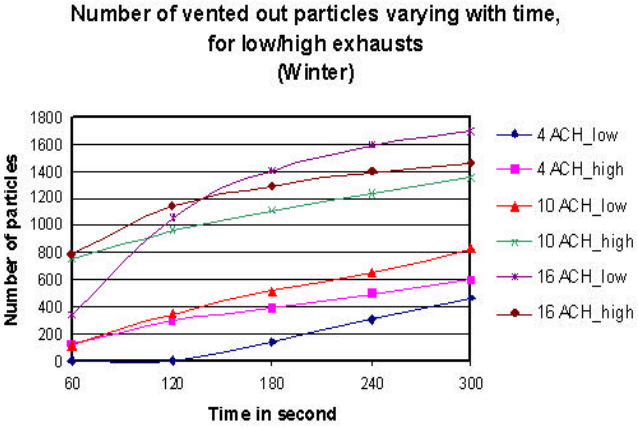

Figure 11 *Number of vented out particles with exhaust location change (winter).*

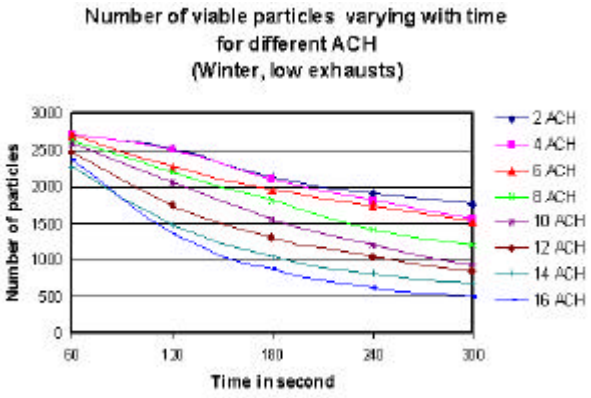

Figure 12 *Number of viable particles with ACH change (winter).*

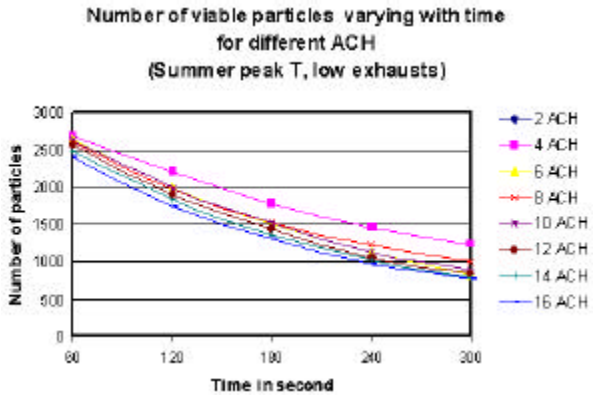

Figure 13 *Number of viable particles with ACH change (summer).*

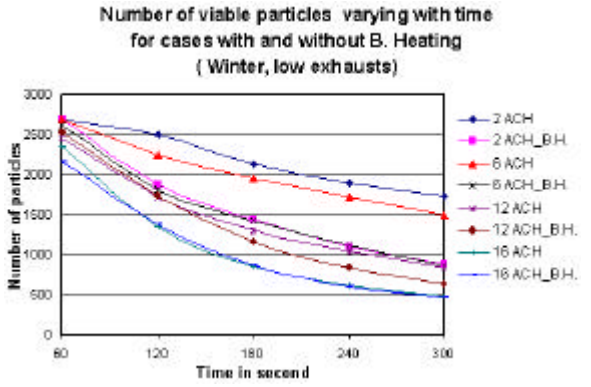

Figure 14 *Number of viable particles with/without baseboard heating.*

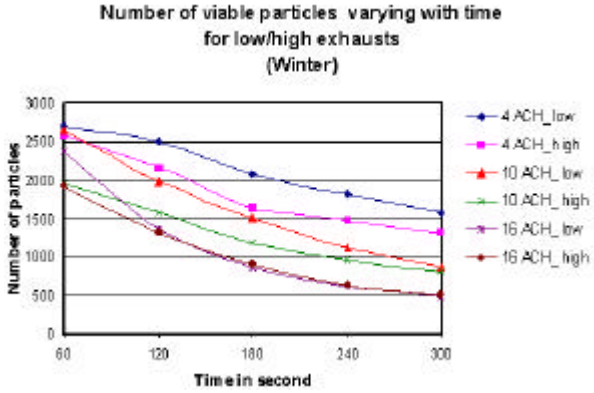

Figure 15 *Number of viable particles with exhaust location change (winter).*

little benefit in increasing the ACH beyond 6 ACH—the curves for this case and that of the 12 ACH case are very similar. In the patient room study, a value of 6 ACH was found to provide very good thermal comfort and uniformity for winter cases with baseboard heat.

The effect of exhaust location on selected winter cases is displayed in Figure 15. The results show that the high exhaust is generally more effective than the low exhaust for the particle release points considered in this study with the exception again being the higher ACH.

Number of Killed Particles Varying with Time

Figures 16 and 17 show the number of killed particles varying with time for ACH. They display the variation for winter (with no baseboard heating) and summer conditions, respectively. The number of particles killed by the UV are generally higher for the summer cases than for the winter cases.

The interesting aspect to these results is that the high ACH does not result in better particle killing by UV beam. The best ventilation rates seem to fall in the range of 10-12 ACH for winter and seem to be at 6 ACH for summer with the UVGI location being studied. The reason for this is that as the ACH is increased, the particles tend to spend less time in the UV zone, leading to lower killing rates.

Survival Fraction of Particles Varying with Time

Figures 18 and 19 show the survival fraction for viable particles varying with time for several parametrical changes. Figures 18 and 19 show the variation with ACH for the summer and winter (with and without baseboard heating) conditions, respectively.

The summer cases (Figure 18) indicate that there is no real variation in survival fraction with ACH—all values are equally as effective. The survival percentage for all these cases is around 80% to 85%, indicating a consistent advantage in the inclusion of UV lamps in the room.

Figure 19 shows the effect of including baseboard heating for selected winter cases. The plot shows further evidence of the advantages in using baseboard heating in winter cases at low ACH.

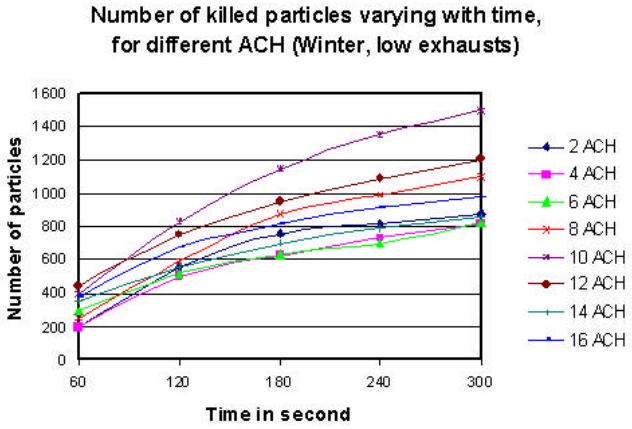

Figure 16 *Number of killed particles with ACH change (winter).*

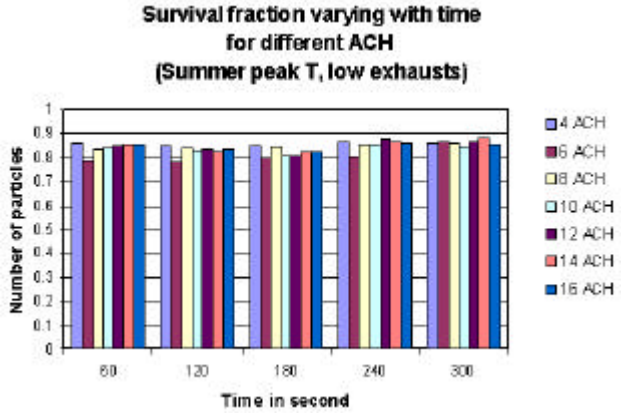

Figure 18 *Survival fraction with ACH change (summer).*

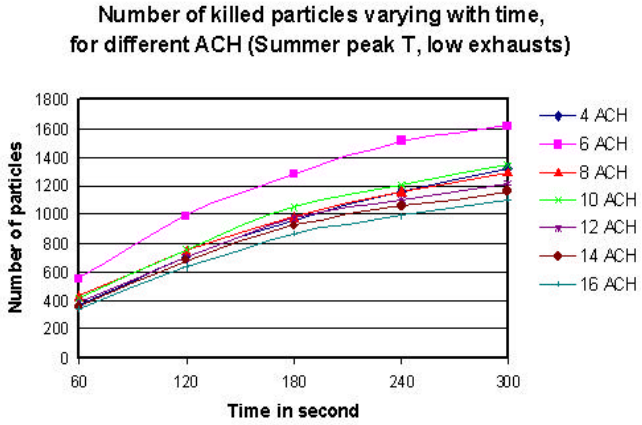

Figure 17 *Number of killed particles with ACH change (summer).*

UV Kill/ Ventilation Percentages for Different UV Locations and Intensity

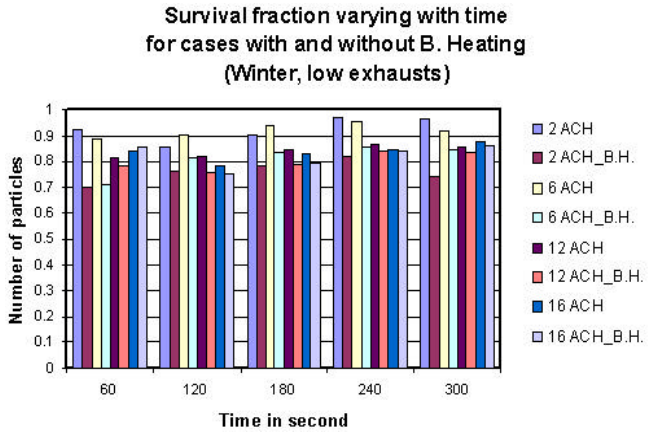

Figure 19 *Survival fraction with/without baseboard heating.*

Figures 20 and 21 compare the number of killed and vented out particles after 300 s with different ventilation flow rates for winter and summer conditions, respectively. The winter plots show that there is an increase and then a reduction in the number of killed particles with increasing ACH. For the summer case, there is a general reduction in the number of killed particles with increasing ACH. The reason for this is that as the ACH is increased and mixing is improved, the particles spend less time in the UV zone.

Figures 22 to 24 show the percentage of particles removed by UV killing and ventilation for different lamp locations and intensities. In particular, two locations were considered, namely, the default position on the vestibule wall and immediately above the bed. Further, three intensities were considered, the original 10 W UV output and also 20 W and 40 W outputs. The designation is clear in the figure title.

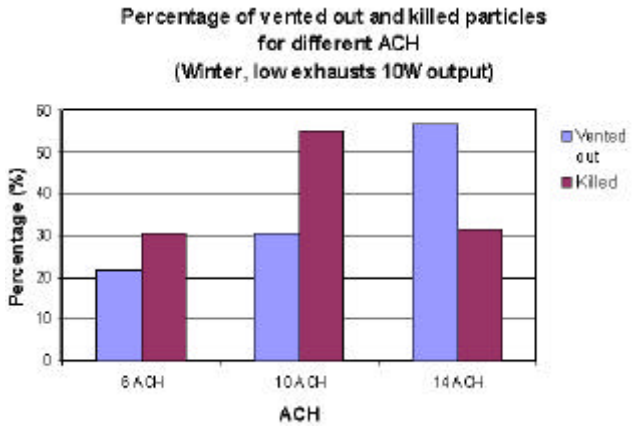

Figure 20 *Comparison of killed and vented particles at 300 s for winter condition.*

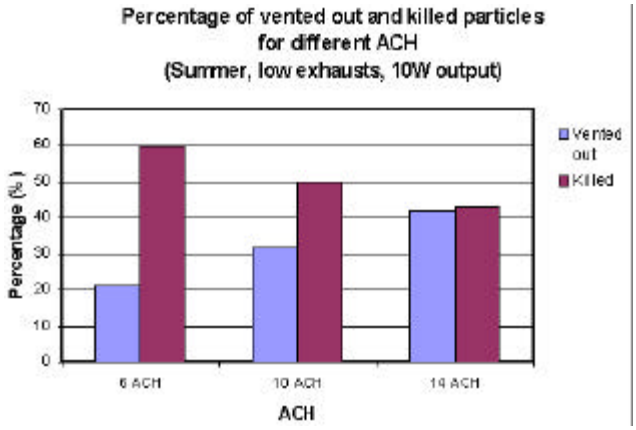

Figure 21 *Comparison of killed and vented particles at 300 s for summer condition.*

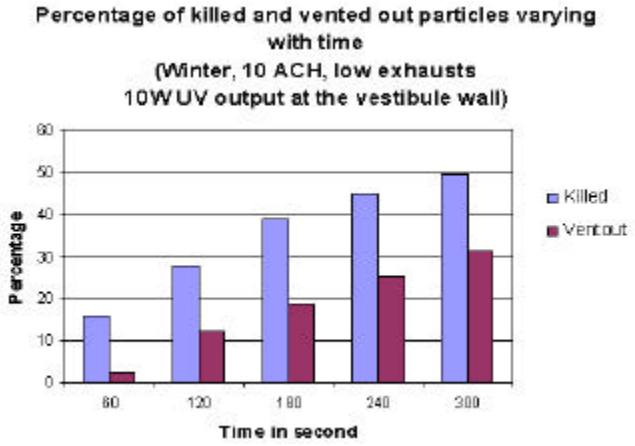

Figure 22 *Killed/vented particle percentages: UV lamp on vestibule wall, 10 W UV output.*

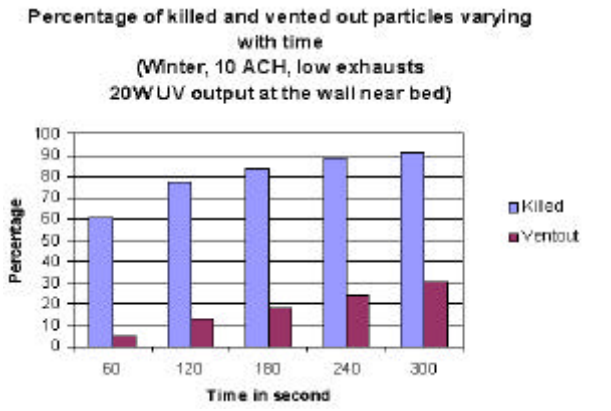

Figure 23 *Kileed/vented particle percentages: UV lamp on wall above patient, 20 W UV output.*

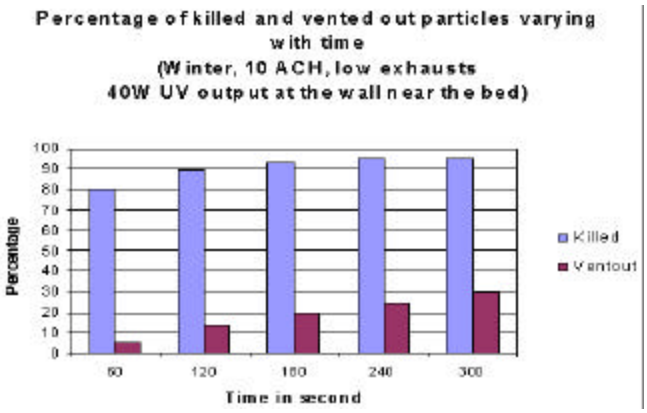

Figure 24 *Killed/vented particles percentages: UV lamp on wall above patient, 40 W UV output.*

It should be noted that the number of killed plus vented particles can exceed 100%. The reason for this is that the vented total includes both viable and killed particles.

The figures show that, as expected, the number of killed particles significantly increases by locating the lamp immediately above the bed and by doubling the UV output. However, on increasing the lamp intensity still further, there is only a very modest increase in the killed percentage at the end of the 300 s time period. This shows that over the entire time scale considered, there is only marginal benefit in increasing the UV intensity.

Comparison of Stick and Non-Stick Models

Figures 25 and 26 show comparisons of the two wall deposition models in terms of the vented out and killed particles. Figures 25 and 26 illustrate the variation of viable and killed particles varying with time for winter cases, and they show that the difference in the number of viable/killed particles becomes more significant when the ventilation rate is high. This is because of the removal of particles through the third mechanism, wall deposition.

Notes

Note 1. Figures 9 to 11 show the number of particles that have been ventilated via the exhausts in the room varying with time. These particles are not used in the calculation of the average UV dosage for the remaining viable particle population.

Note 2. Figures 12 to 15 show the number of viable particles varying with time. Viable particles are defined as the particles that are

- not vented out and
- not killed by UV.

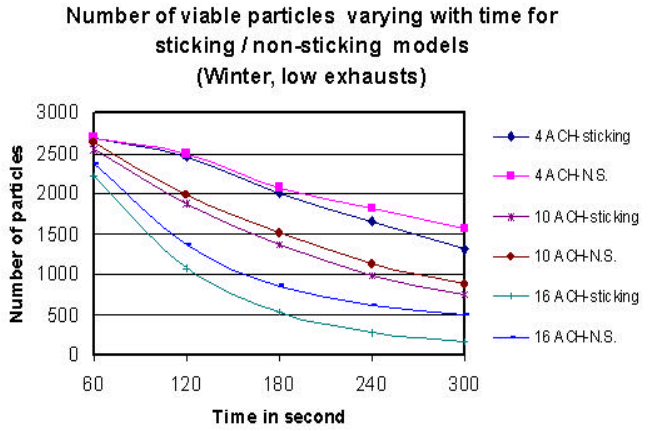

Figure 25 *Number of viable particles varying with time for stick and non-stick models.*

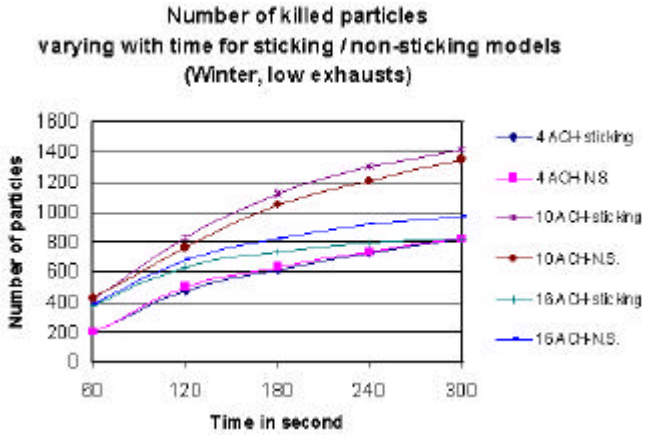

Figure 26 *Number of killed particles varying with time for stick and non-stick models.*

Note that only viable particles contribute to the average UV dose in calculating the percentage of surviving particles.

Note 3. Figures 16 and 17 show the number of killed particles varying with time. The number of particles classed as killed is calculated as follows.

1. The code determines the number of viable particles and records the UV dose (irradiance in $\mu W/cm^2$ × period of exposure in seconds) experienced by each individual particle.
2. At the conclusion of the time interval, an average total dose for the viable particle population is calculated.
3. The average population UV total dose is used as the *It* term in Equation 1 to determine the percentage of survival for the particle population.
4. The number of killed particles is then

Number of killed particles = *Number of viable particles* · (1 – (*survival percentage for population*/100)).

At the beginning of the next time interval, the particles that are tagged as being killed are no longer included in the calculation of the survival percentage. The tagged particles are those that have the highest individual UV total dose.

In order to help understand how the particles are classified, Table 3 lists the particle numbers in different status at the end of every minute for Case 10 (summer, 10 ACH). The summation of airborne, vented out, and wall deposition at the end of any minute is 2700.

- As this calculation is at the end of the first time interval, all particles remaining in the room are assumed to be viable.
- The average UV total dose for the viable particle population is used in the calculation of the survival percentage.
- *Number of killed particles* = *Number of viable particles* · (1 – (*survival percentage for population*/100))

Number of killed particles = 2638 · (1 – (84/100)) = 421

TABLE 3
Budget Table for 2700 Particles (Case 10)

	End of Min. 1	End of Min. 2	End of Min. 3	End of Min. 4	End of Min. 5
Vented out	62	335	508	675	851
Dead vented out	0	40	74	142	235
Viable	2638 (1)	1984 (4)	1508	1119	875
% Surviving	84 (2)	83	80.8	85.6	85.5
Killed	421 (3)	758	1048	1209	1344

- The summation of viable particles, particles killed in the previous time interval, and vented out particles does not match 2700, the number of total particles from the second interval onwards. This is because the number of vented out particles includes the killed particles as well. If subtracting the dead particles from the vented out number, the conservation of total number particles will be obtained. For example, at the end of minute 3, the

balance shows

1508 (viable) + 758 (killed in the previous minute) + 508 (vented) – 74 (dead-vented) = 2700.

Note 4. Figures 20 to 21 show the survival fraction of the particle population varying with time. The survival fraction is calculated with Equation 16 using steps 1 to 3 in Note 3 above.

DISCUSSION AND SUMMARY

There is no significant body of work that addresses the subject of particle deposition on wall surfaces. Lu et al. (1999) were concerned with the numerical modeling and measurement of aerosol particle distributions in ventilated rooms. There are several differences between the work presented in that study and this current work. In particular, in the Lu et al. study, the particle diameters were much larger compared with those in this paper (1 mm to 5 mm compared with 1 μm here), the effect of turbulence on the particles was not included as it is here, and no internal furniture or blockages were considered. The study concluded that particle deposition was a significant means of particle removal. Byrne et al. (1993) showed in an experimental study of aerosol particle deposition in furnished and unfurnished rooms that the deposition rates in the furnished room are much larger than in the unfurnished for the same particle size.

Consensus opinion is that for the particle size considered here, deposition should be around 1%-15%. In this study, particle depositions peaked at around 36% for peak summer cases. As noted in the section "Model for Impingement of Particles on Solid Surfaces," a probability should be introduced when a particle strikes a surface as to whether it sticks or not. The true deposition rate, therefore, falls somewhere between the stick and non-stick models. However, irrespective of whether the stick or non-stick model is considered, similar conclusions can be drawn.

With the above caveat, the results from the cases studied show:

- The number of particles vented out of the room increases with ACH. The variation with ACH is more pronounced for winter cases with no baseboard heating than for summer cases because low ACH cases have poorer mixing.
- Cases with high exhaust grilles vent out more particles than low exhaust systems for the particle release points considered in this study for the low to medium ACH values considered. This trend is not present at the higher values of ACH considered.
- The number of viable particles parameter clearly shows the advantages of using baseboard heating, especially when the ventilation flow rate is low. The results show that there is little advantage in increasing the ventilation rate in the room beyond 6 ACH for summer cases or winter cases with baseboard heating in terms of increasing the effectiveness of the UVGI. This value is also consistent with the results of a concurrent study examining thermal comfort and uniformity in patient rooms (Memarzadeh and Manning 2000). In particular, this study suggests that the optimum ventilation rate for similar winter conditions as considered here is 6 ACH to provide good levels of thermal comfort and uniformity. This value is also suitable for summer condition cases.
- The number of viable particles in the room is generally lower for high exhaust systems compared with low exhaust system cases for the low to medium ACH values considered.
- For the effectiveness of UVGI, the best ventilation rates seem to fall in the range of 10-12 ACH for winter (no baseboard heating) and to be at 6 ACH for summer with the UVGI location being studied.
- UVGI does result in the killing of a significant percentage of the viable particles in the room. In particular, as seen by the Table 3 example, UVGI kills around 50% of the particles in the room.
- Changing the location of the UV lamp and increasing its intensity result in a higher percentage of particles being killed. However, further increases in UV intensity show diminishing returns.
- The addition of baseboard heating results in better UVGI kill rates irrespective of ACH. Baseboard heating should, therefore, be used in winter cases, especially at low ACH.
- The winter plots show that there is an increase and then a reduction in the number of killed particles with increasing ACH. For the summer case, there is a general reduction in the number of killed particles with increasing ACH. The reason for this is that as the ACH is increased and mixing is improved, the particles spend less time in the UV zone.

While the emphasis here has been on the use of UV, if UV not included, the reader can ignore the UV effects and just focus on the ventilation effects. Also, some of the conclusions listed above will still be applicable.

- Baseboard heating should be used in winter cases to improve mixing in the room. This reduces the influence of ACH.
- High level exhausts are generally better than low level exhausts in terms of vented percentage, particularly at low to medium ACH. Note, however, that patient rooms display better air conditions for low exhausts at low to medium ACH (Memarzadeh and Manning 2000).

For a complete listing of all the results in this study, please visit http://des.od.nih.gov/farhad/index.htm.

REFERENCES

Alani, A., D. Dixon-Hardy, and M. Seymour. 1998. Contaminants transport modelling. *EngD in Environmental Technology Conference.*

Byrne, M.A., C. Lange, A.J.H. Goddard, and J. Reed. 1993. Indoor aerosol deposition measurements for exposure assessment calculations. *Indoor Air'93* 13: 415-419.

Chang, J.C., S.F. Ossoff, D.C. Lobe, M.H. Dorfman, R.G. Quall, and J.D. Johnson. 1985. UV inactivation of pathogenic and indicator microorganisms. *All. Environ. Microbiol.* 49: 1361-1365.

Chen, P.-P., and C.T. Crowe. 1984. On the Monte-Carlo method for modelling particle dispersion in turbulence gas-solid flows. *ASME-FED* 10: 37-42.

Federal Register. 1993. Draft guidelines for preventing the transmission of tuberculosis in health-care facilities, 2d ed., notice of comment period. Vol. 58, no. 195.

First, M.W., E.A. Nardell, W. Chaisson, and R. Riley. 1999. Guidelines for the application of upper-room ultraviolet germicidal irradiation for preventing transmission of airborne contagion—Part I: Basic principles. *ASHRAE Transactions* 105 (1): 869-876.

FV. 1995. *FLOVENT® reference manual 1995*. Flomerics, FLOVENT/RFM/0994/1/1.

Gosman, D., and E. Ioannides. 1981. Aspects of computer simulation of liquid-fuelled combustors. *AIAA 19th Aerospace Science Meeting 81-03-23*, pp. 1 - 10.

Haghighat, F., Z. Jiang, and Y. Zhang. 1994. Impact of ventilation rate and partition layout on VOC emission rate: time-dependent contaminant removal. *International Journal of Indoor Air Quality and Climate* 4: 276-283.

Jiang, Z., F. Haghighat, and Q. Chen. 1997. Ventilation performance and indoor air quality in workstations under different supply air systems: A numerical approach. *Indoor + Built Environment* 6: 160-167.

Jiang, Z., Q. Chen, and F. Haghighat. 1995. Airflow and air quality in large enclosures. *ASME Journal of Solar Energy Engineering* 117: 114-122.

Lu, W., A. Howarth, N. Adams, and S. Riffat. 1999. CFD modeling and measurement of aerosol particle distributions in ventilated multizone rooms. *ASHRAE Transactions* 105 (2): 116-127.

Macher, J.M., L.E. Alevantis, Y.-L. Chang, and K.-S. Liu. 1992. Effect of ultraviolet germicidal lamps on airborne microorganisms in outpatient waiting room. *Appl. Occ. Environ. Hyg.* 7: 505-513.

Memarzadeh, F. 1998. *Ventilation design handbook on animal research facilities using static microisolators.* Bethesda: National Institutes of Health, Office of the Director.

Memarzadeh, F., and A. Manning. 2000. Thermal comfort, uniformity and ventilation effectiveness in patient rooms: Performance assessment using ventilation indices. *ASHRAE Transactions* 106 (2).

Mortimer, V.D., and R.T. Hughes. 1995. The effects of ventilation configuration and flow rate on contaminant dispersion. American Industrial Hygiene Association Conference and Exposition.

Ormancey, A., and J. Martinon. 1984. Prediction of particle dispersion in turbulent flow. *PhysicoChemical Hydrodynamics* 5: 229-224.

Press, W.H., S.A. Teukolsky, W.T. Vetterling, and B.P. Flannary. 1992. *Numerical recipes in FORTRAN*, 2d ed. Cambridge: Cambridge University Press.

Shuen, J.-S., L.-D. Chen, and G.M. Faeth. 1983. Evaluation of a stochastic model of particle dispersion in a turbulent round jet. *AIChE Journal* 29: 167-170.

Snyder, W.H., and J.L. Lumley. 1971. Some measurement of particle velocity autocorrelation functions in turbulent flow. *J. Fluid Mechanics* 48: 41-71.

Wallis, G.B. 1969. *One dimensional and two phase flow*. New York: McGraw-Hill.

DISCUSSION

Paul Ninomura, Project Engineer, Indian Health Services, Seattle, Washington: Does your research address isolation rooms without UVGI? Does your research provide recommendations for ACH for an isolation room without UVGI, and if so, what are those recommendations?

Farhad Memarzadeh: As noted in the Discussion and Summary of the paper, the reader can ignore the UV effects and just focus on the ventilation effects. The Discussion and Summary indicates two conclusions that can be applied directly because the UV field applied will not markedly affect the flow field, as the power dissipation from the UVGI is small in comparison with the other heat sources in the room.

Xudong Yang, Assistant Professor, University of Miami, Coral Gables, Florida: Thanks for the interesting results. It seems to me the results are obtained exclusively from numerical simulations. Have you done or are you planning to do experimental measurements to validate the numerical results (in particular, a comparison between the measured and simulated bacteria is very interesting).

You mentioned that the UV can be very effective in killing the bacteria. Is there any negative effect in using such a device in a patient room?

Memarzadeh: The question of bacteria killing by UV was addressed experimentally by investigators other than the authors and published by ASHRAE, as mentioned in the paper.

Excessive exposure, especially direct eye exposure, to the UV radiation will certainly be harmful and, therefore, needs to be prevented. However, the UVGI lamp considered here is located at 7.5 ft above floor level, well away from patient range. New fixture designs with louver and reflectors have been proposed to reflect and focus the radiation to further reduce overexposure in the occupied zone. Exposure to UV will be far less is identified in the standards.

John Lewis, Consulting Engineer, John Lewis and Associates, Pasadena, Calif.: Did you investigate multiple glaz-

ing or high performance (e.g., slot) diffusers adjacent to the window as an alternative to baseboard heating which may be expensive?

Memarzadeh: The window considered here was double glazed, such that only 33% of the incident flux was transmitted. While only one slot diffuser near the window was used in this study, another recent study (Memarzadeh and Manning 2000), indicated that there was not much benefit from using different slot diffuser designs. In both studies, the baseboard heater was found to be by far the most effective device in terms of mixing.